

Decoherence induced deformation of the ground state in adiabatic quantum computation

Qiang Deng,¹ Dmitri V. Averin,¹ Mohammad H. Amin,^{2,3} and Peter Smith^{2,3}

¹*Department of Physics and Astronomy, Stony Brook University, SUNY, Stony Brook, NY 11794-3800*

²*D-Wave Systems Inc., 100-4401 Still Creek Drive, Burnaby, B.C., Canada V5C 6G9*

³*Department of Physics, Simon Fraser University, Burnaby, British Columbia, Canada V5A 1S6*

Adiabatic quantum computation (AQC) [1, 2], either in its universal form [3, 4], or in the form of adiabatic quantum optimization [5, 6], or quantum simulations [7], presents a viable alternative to gate-model quantum computation (GMQC). Although a part of the original motivation for introduction of the AQC [2] was the promise of the increased stability against decoherence due to the energy gap between the ground and excited states, the question of the role of decoherence in AQC remains an open one. This uncertainty makes it important to quantify more precisely the decoherence properties of AQC. A crucial step towards this would be to define a quantitative characteristic of the decoherence strength in AQC, that plays a role similar to the decoherence time for GMQC. However, in the case of AQC, decoherence has qualitatively different, static effect on the qubits, not limiting the operation time of an algorithm [8]. In this work, we propose the ground state fidelity, defined as the distance between the open and closed system reduced density matrices normalized to the Boltzmann ground state probability, as a quantitative measure of decoherence-induced deformation of the ground state in AQC, analogous to the decoherence time for GMQC. We calculate the fidelity perturbatively at finite temperatures and express it through the same environmental noise correlators that determine the decoherence times in GMQC. We discuss the relation between fidelity and the relaxation and dephasing times of the qubits, and its projected scaling properties with the number of qubits.

In AQC, adiabatic evolution of the ground state of a qubit system realizes the solution of a computational problem represented by an appropriately designed Hamiltonian, which is typically written as

$$H_S = A(s)H_U + B(s)H_P, \quad (1)$$

where $s = t/t_f$ with t_f being the total evolution time. At $s = 0$, one has $A(0) = 1$, $B(0) = 0$, and the system is initialized in the ground state of the Hamiltonian H_U , which usually consists of the uniform superposition of all computational basis states. The energy scales $A(s)$ and $B(s)$ are varied monotonically so that at $s = 1$, $A(1) = 0$ and $B(1) = 1$. If the evolution is slow enough, an isolated qubit system stays in the ground state with high fidelity throughout the evolution, and at $s = 1$ reaches the ground state of H_P , which provides a solution to a computational problem.

If the qubit system is weakly coupled to a dissipative environment, two effects are expected. First, the low-frequency part of the environmental noise moves the system energy levels relative to each other. This results in a dephasing of the energy eigenstates that eventually suppresses all off-diagonal elements of the qubit density matrix in the energy basis. However, since the population of the ground state is the only important part of the computation and the relative phases of the energy eigenstates do not carry any information, this does not affect AQC. Second effect of the coupling to the environment is that it induces the thermal transitions between the qubit energy levels pushing the qubit system towards thermal equilibrium at a temperature T . For slow evolution, the instantaneous probability to be in the ground state is given approximately by the Boltzmann distribution, and

so the qubit system loses some of the ground state probability due to thermal occupation of the excited states. Such a thermal loss of probability can be compensated by multiple iterations of an AQC algorithm as long as it does not scale exponentially with the size of the system, i.e. as long as the number of excited states within roughly the energy $k_B T$ above the ground state does not grow exponentially.

The preceding arguments provide an intuitive explanation for the predicted robustness of AQC against local environmental noise in the limit of weak coupling [8–15]. When the strength of the coupling to the environment is increased without changing either the Hamiltonian or the temperature, the qubit Boltzmann distribution is still not directly affected. However, it is known that the decoherence time of the qubits decreases with increased coupling, and strong coupling to the environment eventually makes the qubits completely incoherent, rendering them useless for quantum computation. In GMQC, qubit decoherence leads to computation errors which, without error correction, completely destroy the computation process. This is why the qubits' quality factor, which is the ratio of the decoherence time and the gate operation time, provides a good measure of the qubit performance in GMQC. It is, however, unclear how an increase in coupling to the environment, or equivalently decrease in qubit quality factor, affects AQC.

In this paper, we look closely at what happens to the eigenstates of the qubit system in AQC when coupling to the environment is non-negligible. To ensure consistent notation throughout this paper, symbols with (without) “ \sim ” denote quantities related to the coupled (uncoupled) qubit system and environment. We use letters m, n to

enumerate the eigenstates and eigenvalues of the qubits (e.g., $|n\rangle$, E_n), letters ν, μ to enumerate the eigenstates and eigenvalues of the environmental degrees of freedom, and letters a, b to enumerate the eigenstates and eigenvalues of the *total* system (qubits+environment). The total Hamiltonian is $\tilde{H} = H_S + H_B + H_I$, where H_B and H_I are the environment and interaction Hamiltonians, respectively. In the absence of coupling, $H_I = 0$, and the eigenstates of the total system are $|a\rangle = |n\rangle \otimes |\nu\rangle$ with eigenvalues $E_a = E_n + E_\nu$. When $H_I \neq 0$, the new eigenstates are $|\tilde{a}\rangle$, which typically are entangled superpositions of the unperturbed states $|a\rangle$. For weak coupling, $|\tilde{a}\rangle$ is very close to $|a\rangle$ and the effect of the environment is thermalization of the qubit system. Once the environment is averaged out, the equilibrium of the total system gives the Boltzmann distribution for the qubits:

$$P_n = \sum_{\nu} \frac{e^{-(E_n + E_\nu)/T}}{Z_S Z_B} = \frac{e^{-E_n/T}}{Z_S}, \quad (2)$$

where $Z_S = \sum_n e^{-E_n/T}$ and $Z_B = \sum_{\nu} e^{-E_\nu/T}$ are the partition functions of the qubit system and the environment.

As the coupling increases, the deviation of $|\tilde{a}\rangle$ from $|a\rangle$ grows. In equilibrium, the density matrix of the total system still has the Boltzmann form $\tilde{\rho}_{SB} = \sum_a \tilde{P}_a |\tilde{a}\rangle \langle \tilde{a}|$, where $\tilde{P}_a = e^{-\tilde{E}_a/T} / \tilde{Z}_{SB}$, with $\tilde{Z}_{SB} = \sum_a e^{-\tilde{E}_a/T}$ being the partition function of the total system. However, the reduced density matrix $\tilde{\rho}_S = \text{Tr}_B[\tilde{\rho}_{SB}]$ of the qubit system alone is no longer given by the Boltzmann distribution. The deviation from the Boltzmann form provides a good qualitative measure of how strongly the eigenstates $|\tilde{a}\rangle$ are deformed in comparison to the unperturbed states.

Quantitatively, we define the ground state fidelity as the Uhlmann fidelity [16] between the reduced density matrix $\tilde{\rho}_S$ and the “ideal” ground state density matrix $\rho_0 = |0\rangle \langle 0|$, normalized to the Boltzmann ground state probability P_0 :

$$F = P_0^{-1/2} \text{Tr} \sqrt{\sqrt{\rho_0} \tilde{\rho}_S \sqrt{\rho_0}} = \sqrt{\tilde{P}_0 / P_0}, \quad (3)$$

where $\tilde{P}_0 = \langle 0 | \tilde{\rho}_S | 0 \rangle$ is the equilibrium probability for the qubits to be in the ideal ground state when coupled to the environment. In the weak-coupling limit, no deformation of the eigenstates is expected. Then $\tilde{P}_0 = P_0$, and Eq. (3) gives $F = 1$. This shows that Eq. (3) correctly separates the effect of the quantum deformation of the ground state, which can be viewed as the result of virtual transitions to the excited states, from the thermal loss of probability. Qualitatively, the effect of the virtual transitions, expressed in F , is different from that of the thermal transitions in two important aspects. First, it persists even at $T = 0$, when all the thermal transitions are suppressed. Second, it depends on the strength of coupling to environment (or decoherence time of the qubits), while thermal equilibrium probabilities only de-

pend on the energy eigenvalues and temperature. Nevertheless, similarly to thermal transitions, the virtual transitions reduce the occupation probability of the ground state by transferring it to the higher-energy states.

We calculate the fidelity (3) perturbatively and relate it to measurable parameters of the qubit system and environment. As appropriate for AQC, we assume that the coupling H_I is weak. This allows us to employ the perturbation theory in H_I around the non-interacting state of the qubit system and the environment with both of them in equilibrium at the same temperature T , i.e., density matrices $\rho_S = \sum_n P_n |n\rangle \langle n|$ and $\rho_B = \sum_{\nu} P_{\nu} |\nu\rangle \langle \nu|$, where P_n and P_{ν} are the Boltzmann probabilities. The reduction of the ground state probability due to finite H_I is caused by a change δP_0 in the equilibrium probability P_0 as a result of renormalization of the energy eigenvalues (Lamb shifts), and probability transfers into and out of the ground state due to renormalization of the wavefunctions. The probability \tilde{P}_0 that defines the fidelity (3) can be expressed as

$$\tilde{P}_0 = \text{Tr}_{B,S} \left[|0\rangle \langle 0| \sum_a \tilde{P}_a |\tilde{a}\rangle \langle \tilde{a}| \right]. \quad (4)$$

Introducing interaction-induced corrections to the equilibrium probabilities $\tilde{P}_a = P_a + \delta P_a$, where $P_a = P_n P_{\nu}$, and wavefunctions: $|\tilde{a}(n, \nu)\rangle = |n\rangle \otimes |\nu\rangle + |\delta \tilde{a}(n, \nu)\rangle$, we can rewrite this expression to the lowest non-vanishing order in H_I as

$$\tilde{P}_0 = \delta P_0 + \sum_n P_n \text{Tr}_{B,S} \left[|0\rangle \langle 0| \otimes \rho_B \cdot |\tilde{a}(n, \nu)\rangle \langle \tilde{a}(n, \nu)| \right]. \quad (5)$$

Using the relation $|0\rangle \langle 0| = 1 - \sum_{m \neq 0} |m\rangle \langle m|$ to transform the $n = 0$ term in Eq. (5) we obtain

$$\tilde{P}_0 = P_0 + \delta P_0 - \sum_{n \neq 0} (\Gamma_{0n} P_0 - \Gamma_{n0} P_n), \quad (6)$$

where

$$\Gamma_{mn} \equiv \langle n | \text{Tr}_B [|\delta \tilde{a}(m, \nu)\rangle \langle \delta \tilde{a}(m, \nu)| \rho_B] | n \rangle.$$

The terms proportional to Γ in Eq. (6) describe the reduction of the ground state probability as a result of renormalization of the qubit system wavefunctions by their interaction with the environment.

Next, we calculate δP_0 and Γ_{mn} . Quite generally, the interaction Hamiltonian H_I is

$$H_I = \sum_{j,\alpha} q_j^{\alpha} \sigma_j^{\alpha}, \quad (7)$$

where σ_j^{α} are the Pauli matrices for the j th qubit, $\alpha = x, y, z$, and q_j^{α} are the corresponding operators of the noise generated by the environment. As usual, the averages of the noise operators vanish, $\langle q_j^{\alpha} \rangle = 0$. Then, in the weak coupling regime, the effect of environment is fully characterized by the noise spectral densities:

$$S_j^{\alpha}(\omega) = \int dt e^{i\omega t} \langle q_j^{\alpha}(t) q_j^{\alpha}(0) \rangle, \quad (8)$$

where $\langle \dots \rangle = \text{Tr}_B\{\rho_B \dots\}$ is the average over the environmental degrees of freedom. For simplicity, we limit our discussion to the most typical case when the noises with different α or j are uncorrelated. It is shown in the supplementary information (SI) that the perturbation expansion in H_I in this situation gives

$$\begin{aligned} \delta P_0 &= -\beta P_0 \sum_{j,\alpha,n,m} (P_n - \delta_{n0}) |\sigma_{j,nm}^\alpha|^2 \int \frac{d\omega}{2\pi} \frac{S_j^\alpha(\omega)}{\omega_{mn} + \omega}, \\ \Gamma_{mn} &= \sum_{j,\alpha} |\sigma_{j,nm}^\alpha|^2 \int \frac{d\omega}{2\pi} \frac{S_j^\alpha(\omega)}{(\omega_{nm} + \omega)^2}, \end{aligned} \quad (9)$$

where $\sigma_{j,nm}^\alpha \equiv \langle n | \sigma_j^\alpha | m \rangle$ and $\omega_{nm} \equiv E_n - E_m$. Substituting (9) into (6) and then into (3), we obtain

$$\begin{aligned} F &= 1 - \beta \sum_{j,\alpha,n,m} |\sigma_{j,nm}^\alpha|^2 \int \frac{d\omega}{4\pi} \frac{S_j^\alpha(\omega)(P_n - \delta_{n0})}{\omega_{mn} + \omega} \\ &\quad - \sum_{j,\alpha,n>0} |\sigma_{j,n0}^\alpha|^2 \int \frac{d\omega}{4\pi} \frac{S_j^\alpha(\omega) - (P_n/P_0)S_j^\alpha(-\omega)}{(\omega_{n0} + \omega)^2}. \end{aligned} \quad (10)$$

Equation (10) is our main result. It is well-defined at $T = 0$, when all thermal excitations are suppressed, i.e., $P_n = 0$ for $n > 0$ and $S_j^\alpha(\omega) \equiv 0$ at $\omega < 0$. Hence, the values of ω around $-\omega_{m0}$, when the denominator in (10) vanishes, do not contribute to the integral. When $T \neq 0$, the divergences that appear at $\omega = -\omega_{m0}$ reflect the fact that environment can also create real thermal excitations of the qubit system. However, the detailed balance relation, $S_j^\alpha(-\omega) = e^{-\beta\omega} S_j^\alpha(\omega)$, ensures that these divergences cancel each other out and Eq. (10) is well-defined also at $T \neq 0$ (see the SI).

Equation (10) is now applied to specific problems. The first example we consider is a typical *individual qubit* with the Hamiltonian

$$H_S = -[\epsilon\sigma^z + \Delta\sigma^x]/2 \quad (11)$$

coupled as in Eq. (7), but only through σ^z , to the environmental noise with spectral density $S(\omega)$ (8). In the usual weak-coupling approximation [see, e.g., Ref. 17], the qubit decoherence time T_2^* is given by

$$\frac{1}{T_2^*} = \frac{1}{2T_1} + \frac{1}{T_\varphi}, \quad (12)$$

where T_1 and T_φ are the relaxation and pure dephasing times, given by

$$T_1^{-1} = (\Delta^2/\Omega^2)[S(\Omega) + S(-\Omega)], \quad (13)$$

$$T_\varphi^{-1} = (\epsilon^2/\Omega^2)S(0), \quad (14)$$

with $\Omega = \sqrt{\Delta^2 + \epsilon^2}$. The standard expressions for the eigenstates of the Hamiltonian (11) reduce Eq. (10) for the fidelity to $F = 1 - \Delta^2 K / 2\Omega^2$, where

$$K = \int \frac{d\omega S(\omega - \Omega)}{2\pi\omega} \left\{ \frac{1 - e^{-\omega/T}}{\omega} - \frac{e^{-\Omega/T} + e^{-\omega/T}}{T(e^{-\Omega/T} + 1)} \right\}. \quad (15)$$

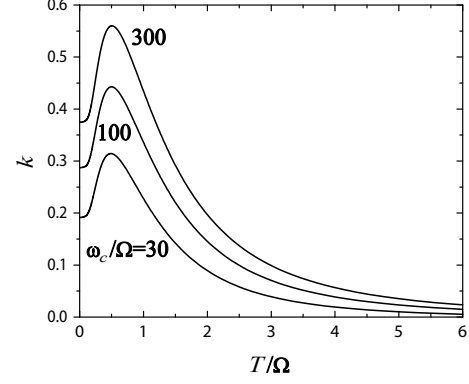


FIG. 1: The temperature-dependent factor k in the expression (17) for the ground state fidelity of an individual qubit in the presence of Ohmic environment with cut-off frequency ω_c .

We see that the same noise spectral density that defines the relaxation and dephasing rates (13) and (14) of the qubits in the GMQC determines the reduction of the ground-state fidelity in AQC. In this respect, the main difference between the reduction of fidelity and the real-time relaxation and dephasing is that even in the lowest-order perturbation theory, the fidelity is reduced by the whole spectrum of environmental excitations, and not just by limited spectral groups resonant with the qubit energy differences or the low-frequency excitations, as in Eqs. (13) and (14).

To strengthen this comparison, we consider an Ohmic bath characterized by the noise

$$S(\omega) = \eta\omega/(1 - e^{-\omega/T}) \quad (16)$$

with cutoff frequency ω_c . In this case, the relaxation time is $T_1^{-1} = \eta(\Delta^2/\Omega) \coth(\Omega/2T)$ and the fidelity is expressed as

$$F = 1 - \frac{k}{Q}, \quad k \equiv \frac{K}{2\eta} \tanh \frac{\Omega}{2T}, \quad (17)$$

where $Q = T_1\Omega$ is the qubit quality factor due to relaxation. Equation (15) gives the following expressions for the factor k at low and high temperatures:

$$k = \frac{1}{4\pi} \begin{cases} \ln(\omega_c/\Omega) - 1 + \pi^2 T^2 / 3\Omega^2, & T \ll \Omega, \\ (\Omega/T)^2 \ln(\omega_c/T), & T \gg \Omega. \end{cases} \quad (18)$$

Equation (17) relates the ground state fidelity to the qubit quality factor, Q , as calculated due to relaxation only. This shows that the fidelity can be related more closely to the relaxation (T_1) and not dephasing (T_φ) processes. Adding a $1/f$ low-frequency noise of a realistic magnitude does not change this conclusion (as discussed in more details in the numerical examples below). As expected, a larger Q leads to a better ground state fidelity. Figure 1 shows the factor k in Eq. (17) as a function of temperature for different cut-off frequencies ω_c . It exhibits the non-monotonic T -dependence, and only weak,

logarithmic, dependence on ω_c , which allows one to estimate the fidelity without precisely specifying ω_c . The factor k is maximal around $k_{\max} \simeq 0.5$ at $T \simeq 0.5\Omega$, which leads to a minimum fidelity $F \simeq 1 - (2Q)^{-1}$. Notice that even a qubit quality factor as low as $Q = 10$, which is practically useless for GMQC, leads to $F > 95\%$ ground state fidelity.

We now consider *multi-qubit systems*, starting with a system of N *uncoupled* qubits. In this case, the trace in the definition of fidelity (3) can be taken independently over separate qubits, so that the total fidelity F is the product of fidelities F_j , $j = 1, \dots, N$ of the individual qubits: $F = \prod_j F_j$. For instance, a typical starting point of AQC algorithms is to initialize the system in the ground state of the Hamiltonian H_U (20). Then, the state of all qubits is the same and can be characterized by the same fidelity (17). Then,

$$F = (1 - k/Q)^N \Big|_{Q \gg k} \simeq e^{-kN/Q}. \quad (19)$$

For independent qubits, fidelity scales exponentially with N as a result of the exponential scaling of the probability for all qubits to remain in their corresponding ground states. Since Q is inversely proportional to the noise strength η , by decreasing the noise by a factors of, e.g., 10, one can achieve the same fidelity with 10 times more qubits.

Next, we focus on how the ground state fidelity behaves in practical AQC systems. We use as an example the *D-Wave One* quantum annealing processor installed at the University of Southern California (see Ref. 6). The Hamiltonian implemented by the processor has the form of Eq. (1), with

$$H_U = - \sum_{i=1}^N \sigma_i^x, \quad H_P = \sum_{i=1}^N h_i \sigma_i^z + \sum_{i,j=1}^N J_{ij} \sigma_i^z \sigma_j^z, \quad (20)$$

where h_i and J_{ij} are tunable dimensionless bias and coupling coefficients. The parameters $A(s)$ and $B(s)$ for this processor are plotted in Fig. 2b. We calculate fidelity of the ground state for a ferromagnetic chain (illustrated in Fig. 2a) with $h_i=0$ and $J_{i,i+1} = -1$, otherwise known as a quantum Ising model in a transverse field. Here, the length of the chain is varied from $N=2$ to 16. Although this model is exactly solvable (see, e.g., Ref. 20 and references therein), fidelity cannot be calculated exactly for practical noise models in which the coupling to environment is dominated by the σ_j^z terms. Hence, we calculate the fidelity numerically. In the limit $N \rightarrow \infty$, the model is known to have a *quantum critical point* at $A(s)=B(s)$. At this point, the chain goes through a quantum phase transition between paramagnetic and ferromagnetic phases. In the ferromagnetic phase, the ground state is doubly degenerate with respect to simultaneous change of signs of all σ_i^z terms. Figure 2c plots several of the lowest energy levels of a 10-qubit chain relative to the ground state energy E_0 . As seen in this plot, the quantum critical point manifests itself as the

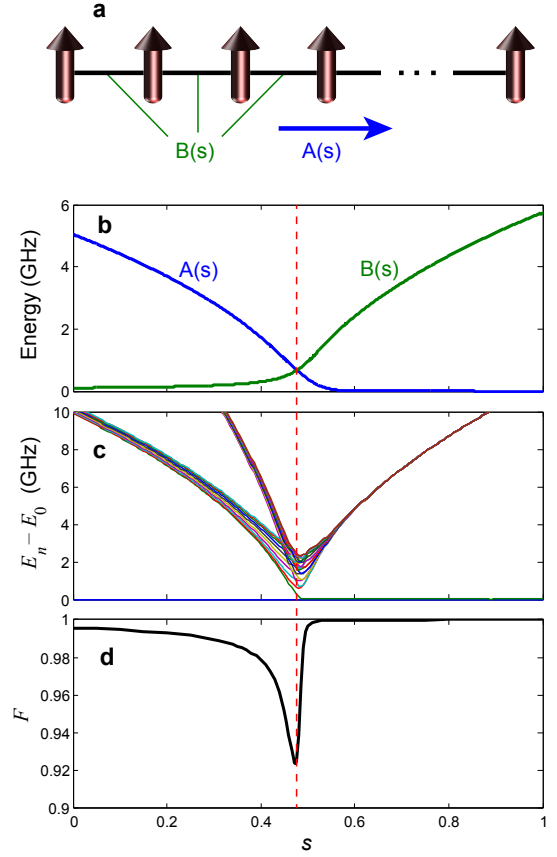


FIG. 2: **a.** A ferromagnetic spin chain with transverse field and coupling energies given, respectively, by $A(s)$ and $B(s)$ in Eq. (1). **b.** Energy scales $A(s)$ and $B(s)$ extracted from experimental parameters. **c.** The lowest 20 energy levels, relative to the ground state, of a 10-qubit ferromagnetic chain with $J_{ij} = -1$, as a function of the normalized time s . **d.** Ground state fidelity of the 10-qubit chain of **c** at $T = 20$ mK. The vertical (red) dashed line marks the quantum critical point.

appearance of the doubly-degenerate ground state and the minimum in the energy gap between the ground and the second excited states.

To calculate fidelity for this system, we use a realistic noise model relevant to the *D-Wave* qubits [18]. In this case, the dominant environmental coupling is to the magnetic flux noise, which couples directly to the qubit computational basis states represented by the σ_j^z operators. The noise spectral density $S(\omega)$ was characterized in the earlier experiments, which were consistent with the noise being a combination of the $1/f$ low-frequency noise and an Ohmic noise at high frequencies [19]. For calculations of fidelity, we take $S(\omega) = \kappa(s)[S_{HF}(\omega) + S_{LF}(\omega)]$, where $S_{HF}(\omega)$ is the Ohmic spectral density (16) and $S_{LF}(\omega) = \gamma^2/|\omega|$. The coefficient $\kappa(s) = B(s)/B(s_m)$ appears because the strength of coupling to flux noise depends on the persistent current of the flux qubits which changes as a function of s (see SI). Here s_m is the bias

point at which the measurements of η and γ are performed. Based on the experimental data, we use $\eta = 0.1$, $\gamma = 20$ MHz and $s_m = 0.636$. We also assume $\omega_c = 100$ GHz for the high-frequency cutoff and $\omega_L = 1$ MHz for the low-frequency cutoff (based on a $t_f \sim 1$ μ s evolution time of an algorithm). We found that for these parameters, the fidelity is dominantly determined by the high-frequency Ohmic noise and not by the $1/f$ noise.

In principle, since the total number of energy levels grows exponentially with N , the time required for numerical calculation of F also grows exponentially. Fortunately, the value of F converges rapidly for a finite number of retained energy states. Here, we keep all energy levels for $N \leq 10$, and up to 2000 energy levels for larger chains. The fidelity of the 10-qubit chain is plotted as a function of s in Fig. 2d. The ground state fidelities of chains with other lengths (and coupled systems other than chains) are qualitatively the same as the one plotted in Fig. 2d. It is clear from the figure that the fidelity is minimum close to the critical point. Notice also that the fidelity approaches $F = 1$ as s increases, which is the result of H_P commuting with H_I , with only σ_j^z terms and negligible other types of coupling to environment. This again reflects the fact that the fidelity depends rather on relaxation than dephasing.

Figure 3 shows the numerical results for the ground state fidelity for N -qubit chains with $N = 1$ to 16 at the critical point. For all chain lengths, the fidelity is better than 90%. It should be emphasized that these are the minimum fidelities at the quantum critical point. The fidelity at all other points is larger, and near $s = 1$, is very close to 1 as shown in Fig. 2d. We have also plotted in Fig. 3 the ground state fidelity of N uncoupled qubits at different N based on the exponential scaling of Eq. (19). The scaling and magnitude of the fidelity at large N is better for the ferromagnetic chain than for the uncoupled qubits. Unfortunately, it was not possible to pursue numerical calculations beyond 16 qubits, as direct perturbation approximation would break down when F strongly deviates from unity. A naive exponential extrapolation of the data points to $N = 128$ (representing the worse case) still yields $F = 0.47$, meaning that the eigenstates could retain their quantum properties without error correction for such a large-size system. As in uncoupled qubits, if one can reduce the noise by a large factor, the size of the chain can be increased by the same factor while keeping the fidelity unchanged. In addition, other techniques such as dynamical decoupling [21] or error correction [22] could be employed to enhance the ground state fidelity at large scales.

Finally, we discuss how the ground state fidelity should affect the performance of AQC. In universal AQC [3, 4], the fidelity of the final ground state determines the quality of the computation. Indeed, deviations of F from 1 mean that the statistics of measurements done on this state will be different from the one that corresponds to the ideal ground state. For instance, in the case of one qubit with $\epsilon = 0$ and the Hamiltonian (11), measurement

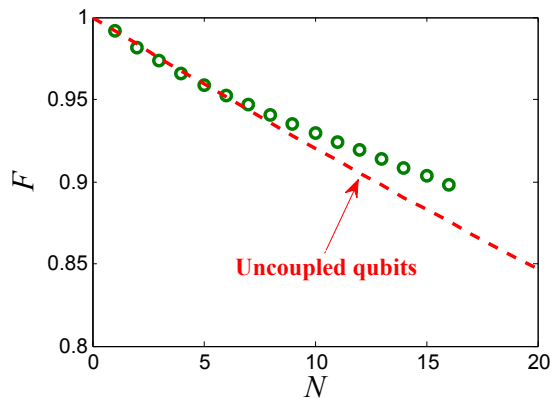


FIG. 3: Ground state fidelity at the quantum critical point for ferromagnetic chains with $N = 1$ to 16, at $T = 20$ mK. Circles are the numerical results using (10). The red dashed line is fidelity of uncoupled qubits from (19), with $k = 0.32$ and $Q = 38.4$.

of σ_x has a non-vanishing probability $1 - F^2$ of producing the result $\sigma_x = -1$ different from the ground state $\sigma_x = 1$ even at temperatures $T \ll \Delta$. However, this effect is absent in the special case when the coupling to environment via H_I commutes with the final Hamiltonian H_P , leading to $F = 1$ at the end of evolution, as in the adiabatic quantum optimization discussed above and shown in Fig. 2d. In this case, thermal transitions increase the loss of probability due to small fidelity in the middle of the evolution, thereby decreasing the ground state probability even further ($\tilde{P}_0 = P_0 F^2$). Therefore, the probability will be distributed among the low energy states even more than implied by the thermal equilibrium. Part of the probability can be regained later when the gap is larger and F is closer to 1. However, since the relaxation time becomes exponentially long near the end of evolution, the majority of the probability that is lost may not be gained back, thus leading to smaller probability of success. This makes it important to maintain fidelity close to unity throughout the evolution. We stress that most treatments of AQC based on the weak coupling master equation, e.g., [8, 9, 23], do not take into account the effect of deformation of the eigenstates that is captured by our calculation of the fidelity.

In summary, we have proposed using ground state fidelity as a quantity for measuring the strength of decoherence effects in AQC. Fidelity plays a role similar to decoherence time in GMQC, but takes into account qualitatively different effects of environment on the ground state relevant to AQC. The fidelity is related to the relaxation processes and is relatively insensitive to the dephasing. Our numerical calculations indicate that fidelity close to unity can be achieved with a moderate qubit quality factor, even for large numbers of qubits. Ground state fidelity should be a useful measure of the environment related quality of AQC systems in the context of further work on important topics in AQC such as quan-

tum error correction or the threshold theorem.

MHA is grateful to A.J. Berkley, M.W. Johnson,

D.A. Lidar, R. Liu, T. Mahon, F. Nori, A. Yu. Smirnov, and B. Wilson for discussions and comments.

-
- [1] Farhi, E., Goldstone, J., Gutmann, S., Lapan, J., Lundgren, A., and Preda D. A Quantum adiabatic evolution algorithm applied to random instances of an NP-complete problem, *Science* **292**, 472 (2001).
 - [2] Mizel, A., Mitchell, M.W., and Cohen, M.L. Energy barrier to decoherence, *Phys. Rev. A* **63**, 040302 (2001).
 - [3] Aharonov, D., van Dam, W., Kempe, J., Landau, Z., Lloyd, S., and Regev, O. Adiabatic quantum computation is equivalent to standard quantum computation, *SIAM J. Comput.* **37**, 166 (2007).
 - [4] Mizel, A., Lidar, D.A., and Mitchell, M. Simple proof of equivalence between adiabatic quantum computation and the circuit model, *Phys. Rev. Lett.* **99**, 070502 (2007).
 - [5] Johnson, M.W. *et al.* Quantum annealing with manufactured spins, *Nature* **473**, 194 (2011).
 - [6] Bian, Z., Chudak, F., Macready, W.G., Clark, L., Gaitan F. Experimental determination of Ramsey numbers with quantum annealing, eprint arXiv:1201.1842.
 - [7] Biamonte, J.D., Bergholm, V., Whitfield, J.D., Fitzsimons, J., and Aspuru-Guzik, A. Adiabatic quantum simulators, *AIP Advances* **1**, 022126 (2011).
 - [8] Amin, M.H.S., Truncik, C.J.S., and Averin, D.V. Role of single qubit decoherence time in adiabatic quantum computation, *Phys. Rev. A* **80**, 022303 (2009).
 - [9] Childs, A.M., Farhi, E., and Preskill, J. Robustness of adiabatic quantum computation. *Phys. Rev. A* **65**, 012322 (2001).
 - [10] Roland, J. and Cerf, N.J. Noise resistance of adiabatic quantum computation using random matrix theory, *Phys. Rev. A* **71**, 032330 (2005).
 - [11] Sarandy, M.S., and Lidar, D.A. Adiabatic quantum computation in open systems, *Phys. Rev. Lett.* **95**, 250503 (2005).
 - [12] Tiersch, M., and Schützhold, R. Non-Markovian decoherence in the adiabatic quantum search algorithm, *Phys. Rev. A* **75**, 062313 (2007).
 - [13] Amin, M.H.S., Love, P.J., and Truncik, C.J.S. Thermally assisted adiabatic quantum computation, *Phys. Rev. Lett.* **100**, 060503 (2008).
 - [14] Amin, M.H.S., Averin, D.V., and Nesteroff, J.A. Decoherence in adiabatic quantum computation, *Phys. Rev. A* **79**, 022107 (2009).
 - [15] Lloyd, S. Robustness of adiabatic quantum computing, eprint arXiv:0805.2757.
 - [16] Uhlmann, A., The transition probability in the state space of a $*$ -algebra, *Rep. Math. Phys.* **9**, 273 (1976).
 - [17] K. Blum, *Density matrix theory and applications*, (Plenum, New York, 1981).
 - [18] Harris, R., *et al.* Experimental demonstration of a robust and scalable flux qubit, *Phys. Rev. B* **81**, 134510 (2010).
 - [19] Lanting, T. *et al.* Probing high-frequency noise with macroscopic resonant tunneling, *Phys. Rev. B* **83**, 180502(R) (2011).
 - [20] Dziarmaga J. Dynamics of a quantum phase transition: exact solution of the quantum Ising model, *Phys. Rev. Lett.* **95**, 245701 (2005).
 - [21] Lidar, D.A. Towards fault tolerant adiabatic quantum computation, *Phys. Rev. Lett.* **100**, 160506 (2008).
 - [22] Jordan, S., Farhi, E., and Shor, P. Error-correcting codes for adiabatic quantum computation, *Phys. Rev. A* **74**, 052322 (2006).
 - [23] Albash, T., Boixo, S., Daniel A. Lidar, D.A., and Zanardi P. Quantum adiabatic markovian master equations, eprint arXiv:1206.4197.

SUPPLEMENTARY INFORMATION

In this document, we provide details of the derivation of the main equation for the ground state fidelity and a brief description of the numerical calculations.

I. GROUND STATE FIDELITY

To be consistent with the notation in the main text, we use symbols with (without) “ \sim ” to denote quantities related to the coupled (uncoupled) qubit system and environment. We also use m, n, k to enumerate qubit system’s eigenstates and eigenvalues (e.g., $|n\rangle$, E_n). Similarly, the letters ν, μ correspond to environment eigenstates and eigenvalues, and letters a, b correspond to *total* system (qubits+environment) eigenstates and eigenvalues. The total Hamiltonian is written as $\tilde{H} = H_S + H_B + H_I$, which includes the qubit system Hamiltonian

$$H_S = \sum_n E_n |n\rangle\langle n|, \quad (21)$$

and interaction Hamiltonian

$$H_I = \sum_{\alpha, j} q_j^\alpha \sigma_j^\alpha, \quad (22)$$

where σ_j^α are the Pauli matrices, $\alpha = x, y, z$, and q_j^α are the noise operators dependent on the heat bath variables coupled to the j -th qubit. The bath Hamiltonian H_B is not specified, but the bath is assumed to be in thermal equilibrium at temperature T . For the purpose of perturbative calculations of fidelity in this work, the properties of q_j^α are completely characterized by its spectral density

$$S_j^\alpha(\omega) = \int_{-\infty}^{\infty} dt e^{i\omega t} \langle q_j^\alpha(t) q_j^\alpha(0) \rangle \quad (23)$$

where $q_j^\alpha(t) = e^{iH_B t} q_j^\alpha e^{-iH_B t}$, and vanishing average $\langle q_j^\alpha(t) \rangle \equiv 0$.

Even if the dissipative environment does not excite the system out of its ground state, the non-vanishing H_I term changes the structure of the ground state wavefunction in comparison with the unperturbed ground state of the Hamiltonian H_S . The magnitude of this change can be characterized quantitatively by fidelity. For two general density matrices ρ and ρ' acting on the same Hilbert space, the fidelity (sometimes called Uhlmann’s fidelity) is given by

$$\mathcal{F}(\rho, \rho') = \text{Tr} \sqrt{\sqrt{\rho} \rho' \sqrt{\rho}}. \quad (24)$$

If one of the states is a pure state, e.g., $\rho = |\psi\rangle\langle\psi|$, then we can use the property $\sqrt{\rho} = \rho = \rho^2$ to write

$$\begin{aligned} \mathcal{F}(\rho, \rho') &= \text{Tr} \sqrt{|\psi\rangle\langle\psi| \rho' |\psi\rangle\langle\psi|} = \sqrt{\langle\psi| \rho' |\psi\rangle} \\ &= \{\text{Tr}[\rho \rho']\}^{1/2}. \end{aligned} \quad (25)$$

Let $|a\rangle$ and $|\tilde{a}\rangle$ denote the unperturbed and perturbed states of the total system, respectively. The total density matrix of the combined system is $\rho_{SB} = \sum_a \tilde{P}_a |\tilde{a}\rangle\langle\tilde{a}|$, where \tilde{P}_a is the probability of finding the total system in the state $|\tilde{a}\rangle$. We define the reduced density matrix as $\tilde{\rho}_S = \text{Tr}_B[\rho_{SB}]$, where the partial trace is taken only over the environmental degrees of freedom. We also define the pure state density matrix $\rho_0 = |0\rangle\langle 0|$, where $|0\rangle$ is the ground state of the (isolated) qubit system Hamiltonian H_S . Then, we express the fidelity \mathcal{F} between $\rho_0 = |0\rangle\langle 0|$ and $\tilde{\rho}_S$ as

$$\mathcal{F}(\rho_0, \tilde{\rho}_S)^2 = \langle 0 | \tilde{\rho}_S | 0 \rangle = \tilde{P}_0, \quad (26)$$

where \tilde{P}_0 is the probability of finding the open system in state $|0\rangle$. In equilibrium, this probability is determined by the thermal distribution over the system eigenstates and also by the effects of the non-vanishing coupling to the environment. To separate these two contributions, we define the ground state fidelity as

$$F \equiv P_0^{-1/2} \mathcal{F}(\rho_0, \tilde{\rho}_S) = \sqrt{\frac{\tilde{P}_0}{P_0}}, \quad (27)$$

where $P_0 = e^{-E_0/T}/Z$ is the Boltzmann probability of the ground state $|0\rangle$ with partition function $Z = \sum_n e^{-E_n/T}$ in the case of an isolated qubit system.

II. PERTURBATIVE CALCULATION OF FIDELITY

In the situation relevant to quantum computation, the coupling H_I is weak and can be treated by perturbation theory around the non-interacting state of the qubit system and environment. In the context of AQC, one can also assume that both the qubits and environment are in equilibrium at the same temperature T . These are characterized by the density matrices $\rho_S = \sum_n P_n |n\rangle\langle n|$ and $\rho_B = \sum_\nu P_\nu |\nu\rangle\langle\nu|$ without the interaction, while the total interacting system has the density matrix $\tilde{\rho}_{SB} = \sum_a \tilde{P}_a |\tilde{a}\rangle\langle\tilde{a}|$, where \tilde{P}_a , P_n , and P_ν are the Boltzmann probabilities. The probability \tilde{P}_n of finding the qubit system in the state $|n\rangle$ in the presence of interaction can be written as

$$\tilde{P}_n = \text{Tr}_{B,S}[|n\rangle\langle n| \tilde{\rho}_{SB}]. \quad (28)$$

The interaction H_I creates corrections to the equilibrium probabilities $\tilde{P}_a = P_a + \delta P_a$, where $P_a = P_n P_\nu$, and to the wavefunctions: $|\tilde{a}(n, \nu)\rangle = |a(n, \nu)\rangle + |\delta\tilde{a}(n, \nu)\rangle$, where $|a(n, \nu)\rangle = |n\rangle \otimes |\nu\rangle$. In the lowest non-vanishing order in H_I , one can separate these corrections in the total density matrix of the system:

$$\tilde{\rho}_{SB} = \sum_a [\delta P_a |a\rangle\langle a| + P_a |\tilde{a}\rangle\langle\tilde{a}|]. \quad (29)$$

This expression reduces Eq. (28) for the probability \tilde{P}_n to:

$$\tilde{P}_n = \delta P_n + \sum_m P_m \text{Tr}_{B,S} [|n\rangle \langle n| \otimes \rho_B \cdot |\tilde{a}(m, \nu)\rangle \langle \tilde{a}(m, \nu)|]. \quad (30)$$

Using the relation $|n\rangle \langle n| = 1 - \sum_{k \neq 0} |k\rangle \langle k|$ to transform the $n = m$ term in Eq. (30), we obtain

$$\tilde{P}_n = P_n + \delta P_n - \sum_{m \neq n} (\Gamma_{nm} P_n - \Gamma_{mn} P_m), \quad (31)$$

where

$$\Gamma_{mn} \equiv \langle n | \text{Tr}_B [|\tilde{a}(m, \nu)\rangle \langle \tilde{a}(m, \nu)| \rho_B] | n \rangle. \quad (32)$$

The Γ -factors in (32) represent the fractions of the probability transfer from the state $|m\rangle$ to the state $|n\rangle$ of the qubit system due to renormalization of the qubit system wavefunctions by non-vanishing coupling to the environment. Equation (31) shows that, in addition to these transfers, environment-induced change of the probabilities \tilde{P}_n is also caused by the change in the equilibrium probability δP_n due to renormalization of the energy eigenvalues (Lamb shift).

Next, we calculate these two contributions explicitly using the perturbation expansion. We start with δP_n . As shown below, the changes of the equilibrium occupation probabilities δP_n of the qubits states are determined by the changes δE_a of the total system energies *averaged* over the equilibrium state of the environment. Since $\langle q_j^\alpha \rangle = 0$, the linear corrections to the qubit system energies vanish, and the relevant energy changes are given by second-order perturbation:

$$\delta E_a = \sum_{b \neq a} \frac{|\langle a | H_I | b \rangle|^2}{E_a - E_b} = \sum'_{\alpha, j, m, \mu} \frac{|\sigma_{j, nm}^\alpha|^2 |\langle \nu | q_j^\alpha | \mu \rangle|^2}{\omega_{nm} + E_\nu - E_\mu}. \quad (33)$$

The prime sign over the sum excludes terms with zero denominator. The average change of the qubit system energy eigenvalues due to coupling to the environment, which determines δP_n , is therefore

$$\delta E_n = \sum_\nu P_\nu \delta E_{n, \nu} = \sum'_{\alpha, j, m, \nu, \mu} P_\nu \frac{|\sigma_{j, nm}^\alpha|^2 |\langle \nu | q_j^\alpha | \mu \rangle|^2}{\omega_{nm} + E_\nu - E_\mu}. \quad (34)$$

We express this result in terms of the noise spectral densities. In this calculation, we assume that the noises with different α and j are uncorrelated. The standard spectral decomposition,

$$S_j^\alpha(\omega) = 2\pi \sum_{\nu, \mu} P_\nu |\langle \nu | q_j^\alpha | \mu \rangle|^2 \delta(\omega + E_\nu - E_\mu), \quad (35)$$

transforms Eq. (34) into

$$\delta E_n = \sum_{j, \alpha, m} \int \frac{d\omega}{2\pi} \frac{|\sigma_{j, nm}^\alpha|^2 S_j^\alpha(\omega)}{\omega_{nm} - \omega}. \quad (36)$$

Now, we relate the changes in the occupation probabilities of the qubit states to the energy changes of the total system. Expanding the Boltzmann probabilities, we get

$$\begin{aligned} \delta P_a &= -\beta \frac{e^{-\beta E_a} \delta E_a}{\sum_b e^{-\beta E_b}} + \beta \frac{e^{-\beta E_a} \sum_b e^{-\beta E_b} \delta E_b}{(\sum_b e^{-\beta E_b})^2} \\ &= -\beta P_a \delta E_a + \beta P_a \sum_b P_b \delta E_b \\ &= \beta P_a \sum_b (P_b - \delta_{ab}) \delta E_b. \end{aligned} \quad (37)$$

Using $P_a = P_n P_\nu$, $P_b = P_m P_\mu$, and $\delta_{ab} = \delta_{nm} \delta_{\nu\mu}$, we see that δP_n is indeed determined by the energy shifts averaged over the environment:

$$\begin{aligned} \delta P_n &= \sum_\nu \delta P_a = \beta \sum_\nu P_n P_\nu \sum_{m, \mu} (P_m P_\mu - \delta_{nm} \delta_{\nu\mu}) \delta E_{m, \mu} \\ &= \beta P_n \sum_{m, \mu} (P_m - \delta_{nm}) P_\mu \delta E_{m, \mu} \\ &= \beta P_n \sum_m (P_m - \delta_{nm}) \delta E_m. \end{aligned} \quad (38)$$

Combining Eqs. (36) and (38), we obtain

$$\delta P_n = -\beta P_n \sum_{j, \alpha, m, k} (P_m - \delta_{mn}) |\sigma_{j, mk}^\alpha|^2 \int \frac{d\omega}{2\pi} \frac{S_j^\alpha(\omega)}{\omega_{km} + \omega}. \quad (39)$$

Next, we calculate the probability transfer fractions Γ_{mn} (32). It is convenient to view the relation between the states with and without interaction as arising from the adiabatic switching on of the interaction:

$$|\tilde{a}\rangle = U |a\rangle, \quad (40)$$

where

$$U = \mathcal{T} \exp \left\{ -i \int_{-\infty}^0 dt e^{\lambda t} H_I(t) \right\}. \quad (41)$$

Here λ is a small positive number which ensures an adiabatic increase of the coupling, and

$$\begin{aligned} H_I(t) &= e^{i(H_S + H_B)t} H_I e^{-i(H_S + H_B)t} \\ &= \sum_{\alpha, j, n, m} \sigma_{j, nm}^\alpha e^{i\omega_{nm}t} q_j^\alpha(t) |n\rangle \langle m| \end{aligned} \quad (42)$$

with H_I given by Eq. (22).

Using Eq. (40) together with (41) limited to the lowest order in H_I in Eq. (32), we obtain

$$\begin{aligned} \Gamma_{mn} &= \text{Tr}_B [\langle n | U | m \rangle \rho_B \langle m | U^\dagger | n \rangle] \\ &= \int_{-\infty}^0 dt \int_{-\infty}^0 dt' \text{Tr}_B [\langle n | e^{\lambda t} H_I(t) | m \rangle \rho_B \langle m | e^{\lambda t'} H_I(t') | n \rangle] \\ &= \int_{-\infty}^0 dt \int_{-\infty}^0 dt' \sum_{j, \alpha} |\sigma_{j, nm}^\alpha|^2 e^{\lambda(t+t')} e^{i\omega_{nm}(t-t')} \langle q_j^\alpha(t') q_j^\alpha(t) \rangle. \end{aligned}$$

We combine this expression with Eq. (23) for spectral densities to get

$$\begin{aligned}\Gamma_{mn} &= \sum_{j,\alpha} |\sigma_{j,nm}^\alpha|^2 \int \frac{d\omega}{2\pi} S_j^\alpha(\omega) \\ &\quad \times \int_{-\infty}^0 dt \int_{-\infty}^0 dt' e^{\lambda(t+t') + i(\omega_{nm} + \omega)(t-t')} \\ &= \sum_{j,\alpha} |\sigma_{j,nm}^\alpha|^2 \int \frac{d\omega}{2\pi} \frac{S_j^\alpha(\omega)}{\lambda^2 + (\omega_{nm} + \omega)^2}.\end{aligned}\quad (43)$$

In the limit $\lambda \rightarrow 0$, this gives

$$\Gamma_{mn} = \sum_{j,\alpha} |\sigma_{j,nm}^\alpha|^2 \int \frac{d\omega}{2\pi} \frac{S_j^\alpha(\omega)}{(\omega_{nm} + \omega)^2}.\quad (44)$$

The final result is

$$\begin{aligned}\tilde{P}_n &= P_n - \beta P_n \sum_{j,\alpha,m,k} |\sigma_{j,mk}^\alpha|^2 \int \frac{d\omega}{2\pi} \frac{S_j^\alpha(\omega)(P_m - \delta_{mn})}{\omega_{km} + \omega} \\ &\quad - \sum_{j,\alpha,m \neq n} |\sigma_{j,mn}^\alpha|^2 \int \frac{d\omega}{2\pi} \frac{P_n S_j^\alpha(\omega) - P_m S_j^\alpha(-\omega)}{(\omega_{mn} + \omega)^2}.\end{aligned}\quad (45)$$

This equation gives the normalized fidelity of the ground state $n = 0$ as

$$\begin{aligned}F = \sqrt{\frac{\tilde{P}_0}{P_0}} &= 1 - \beta \sum_{j,\alpha,n,m} |\sigma_{j,nm}^\alpha|^2 \int \frac{d\omega}{4\pi} \frac{S_j^\alpha(\omega)(P_n - \delta_{n0})}{\omega_{mn} + \omega} \\ &\quad - \sum_{j,\alpha,n > 0} |\sigma_{j,n0}^\alpha|^2 \int \frac{d\omega}{4\pi} \frac{S_j^\alpha(\omega) - (P_n/P_0)S_j^\alpha(-\omega)}{(\omega_{n0} + \omega)^2}.\end{aligned}\quad (46)$$

This is our central equation, which is used in the numerical calculations. As shown in the next subsection, it can also be obtained directly from the partition function of the total system. However, the physical interpretation of the following derivation is less transparent than the derivation presented above.

A. Alternative derivation using partition function

Consider the partition function

$$\tilde{Z} = \text{Tr} \left(e^{-\beta \tilde{H}} \right). \quad (47)$$

Using Eq. (21) one can express the occupation probabilities \tilde{P}_n directly through \tilde{Z}

$$\begin{aligned}-\frac{1}{\beta} \frac{\partial}{\partial E_n} \ln \tilde{Z} &= \frac{1}{\tilde{Z}} \text{Tr} \left(e^{-\beta \tilde{H}} \frac{\partial \tilde{H}}{\partial E_n} \right) = \text{Tr} (\tilde{\rho}_{SB} |n\rangle \langle n|) \\ &= \langle n | \text{Tr}_B (\tilde{\rho}_{SB}) |n\rangle = \langle n | \tilde{\rho}_S |n\rangle = \tilde{P}_n\end{aligned}\quad (48)$$

where

$$\tilde{\rho}_{SB} = \frac{e^{-\beta \tilde{H}}}{\tilde{Z}} \quad (49)$$

is the total density matrix of the system plus environment.

First, we calculate the partition function in the interaction representation,

$$e^{-\beta \tilde{H}} = e^{-\beta H} \left(\mathcal{T} \exp \int_0^\beta d\tau H_I(\tau) \right), \quad (50)$$

where $H = H_S + H_B$ is the non-interacting part of the Hamiltonian and $H_I(\tau) = e^{\beta H} H_I e^{-\beta H}$. Therefore,

$$\begin{aligned}\tilde{Z} &= \text{Tr} \left(e^{-\beta \tilde{H}} \right) = \text{Tr} \left[e^{-\beta H} \left(\mathcal{T} \exp \int_0^\beta d\tau H_I(\tau) \right) \right] \\ &= Z \text{Tr} \left[\rho_{SB} \left(\mathcal{T} \exp \int_0^\beta d\tau H_I(\tau) \right) \right] \\ &= Z \left\langle \mathcal{T} \exp \int_0^\beta d\tau H_I(\tau) \right\rangle,\end{aligned}\quad (51)$$

where $\langle \dots \rangle = \text{Tr}[\rho_{SB} \dots]$ and $\rho_{SB} = e^{-\beta H}/Z$ is the density matrix for the non-interacting qubit system plus environment, which has the form $\rho_{SB} = \rho_S \otimes \rho_B = \sum_n P_n |n\rangle \langle n| \otimes \rho_B$, where P_n is the occupation probability of state $|n\rangle$ and ρ_B is the density matrix of the environment alone. Expanding to second order, we have

$$\begin{aligned}\tilde{Z} &= Z \left(1 + \int_0^\beta d\tau \int_0^\tau d\tau' \langle H_I(\tau) H_I(\tau') \rangle \right) \\ &= Z \left(1 + \int_0^\beta d\tau \int_0^\tau d\tau' \langle q_j^\alpha(\tau) q_j^\alpha(\tau') \rangle_B \right. \\ &\quad \cdot \left. \sum_{j,\alpha,n} P_n \langle n | \sigma_j^z(\tau) \sigma_j^z(\tau') | n \rangle \right),\end{aligned}\quad (52)$$

where $\langle \dots \rangle_B = \text{Tr}_B[\rho_B \dots]$. We write the integral in this expression in terms of the environment spectral density using

$$\langle q_j^\alpha(\tau) q_j^\alpha(\tau') \rangle_B = \int \frac{d\omega}{2\pi} S_j^\alpha(\omega) e^{-\omega(\tau - \tau')}. \quad (53)$$

Defining $\sigma_{j,nm}^\alpha = \langle n | \sigma_j^\alpha | m \rangle$ and $\omega_{nm} = E_n - E_m$, we find

$$\begin{aligned}\text{Integral} &= \sum_{j,\alpha,n,m} \int \frac{d\omega}{2\pi} P_n |\sigma_{j,nm}^\alpha|^2 S_j^\alpha(\omega) \\ &\quad \times \int_0^\beta d\tau \int_0^\tau d\tau' e^{i(\omega_{nm} - \omega)(\tau - \tau')} \\ &= \sum_{j,\alpha,n,m} \int \frac{d\omega}{2\pi} P_n |\sigma_{j,nm}^\alpha|^2 S_j^\alpha(\omega) \\ &\quad \times \frac{e^{\beta(\omega_{nm} - \omega)} - 1 - \beta(\omega_{nm} - \omega)}{(\omega_{nm} - \omega)^2} \\ &= \sum_{j,\alpha,n,m} \int \frac{d\omega}{2\pi} \frac{|\sigma_{j,nm}^\alpha|^2}{(\omega_{nm} - \omega)^2} [P_m S_j^\alpha(-\omega) - P_n S_j^\alpha(\omega)] \\ &\quad - \sum_{j,\alpha,n,m} \int \frac{d\omega}{2\pi} \frac{\beta P_n |\sigma_{j,nm}^\alpha|^2 S_j^\alpha(\omega)}{\omega_{nm} - \omega}\end{aligned}\quad (54)$$

In the last step we used $P_m = e^{\beta\omega_{nm}} P_n$, which is valid for the Boltzmann distribution, and $S_j^\alpha(-\omega) = S_j^\alpha(\omega)e^{-\beta\omega}$. The first integral in the last equation vanishes, giving

$$\tilde{Z} = Z \left(1 - \sum_{j,\alpha,n,m} \int \frac{d\omega}{2\pi} \frac{\beta P_n |\sigma_{j,nm}^\alpha|^2 S_j^\alpha(\omega)}{\omega_{nm} - \omega} \right). \quad (55)$$

Therefore,

$$\ln \tilde{Z} = \ln Z + \sum_{j,\alpha,n,m} \int \frac{d\omega}{2\pi} \frac{\beta P_n |\sigma_{j,nm}^\alpha|^2 S_j^\alpha(\omega)}{\omega_{mn} + \omega}, [P_n S_j^\alpha(\omega) - P_m S_j^\alpha(-\omega)]$$

and

$$\begin{aligned} \tilde{P}_n &= -\frac{1}{\beta} \frac{\partial}{\partial E_n} \ln \tilde{Z} = -\frac{1}{\beta} \frac{\partial}{\partial E_n} \ln Z \\ &\quad - \frac{\partial}{\partial E_n} \sum_{j,\alpha,n,m} \int \frac{d\omega}{2\pi} \frac{P_m |\sigma_{j,nm}^\alpha|^2 S_j^\alpha(\omega)}{\omega_{km} + \omega}. \end{aligned} \quad (56)$$

Finally, we transform this equation using the relations

$$\begin{aligned} -\frac{1}{\beta} \frac{\partial}{\partial E_n} \ln Z &= P_n, \\ \frac{\partial}{\partial E_n} \frac{1}{\omega_{km} + \omega} &= \frac{\delta_{mn} - \delta_{kn}}{(\omega_{km} + \omega)^2}, \\ \frac{\partial P_m}{\partial E_n} &= \beta P_n (P_m - \delta_{mn}), \end{aligned} \quad (57)$$

to obtain

$$\begin{aligned} \tilde{P}_n &= P_n - \beta \sum_{j,\alpha,m,k} |\sigma_{j,mk}^\alpha|^2 \int \frac{d\omega}{2\pi} \frac{S_j^\alpha(\omega) P_n (P_m - \delta_{mn})}{\omega_{km} + \omega} \\ &\quad - \sum_{j,\alpha,m \neq n} |\sigma_{j,mn}^\alpha|^2 \int \frac{d\omega}{2\pi} \frac{P_n S_j^\alpha(\omega) - P_m S_j^\alpha(-\omega)}{(\omega_{mn} + \omega)^2}. \end{aligned} \quad (58)$$

This is the same equation as (45). Using (27), one recovers Eq. (46) for fidelity.

III. NUMERICAL CALCULATIONS

In this section, we derive the equations that form the basis of our numerical calculation of the ground state fidelity F . We assume that the noise is coupled only to σ_j^z operators and $S_j^z(\omega) = S(\omega)$ is the same for all qubits. We also define $M_{mn} = \sum_j |\sigma_{j,mn}^z|^2$. Equation (46) can be rewritten as

$$\begin{aligned} F^2 &= 1 - \beta \sum_{m,n>0} M_{mn} \int \frac{d\omega}{2\pi} \frac{S(\omega) P_n}{\omega_{mn} + \omega} \\ &\quad - \beta \sum_{n>0} M_{0n} \int \frac{d\omega}{2\pi} \frac{S(\omega) P_n}{\omega_{0n} + \omega} \\ &\quad - \beta \sum_m M_{m0} \int \frac{d\omega}{2\pi} \frac{S(\omega) (P_0 - 1)}{\omega_{m0} + \omega} \\ &\quad - \sum_{n>0} M_{n0} \int \frac{d\omega}{2\pi} \frac{S(\omega) - (P_n/P_0) S(-\omega)}{(\omega_{n0} + \omega)^2}. \end{aligned} \quad (59)$$

We use $M_{nm} = M_{mn}$ and change ω to $-\omega$ in some integrals to get

$$\begin{aligned} F^2 &= 1 - \beta \sum_{m,n>0} M_{mn} \int \frac{d\omega}{2\pi} \frac{S(\omega) P_n}{\omega_{mn} + \omega} \\ &\quad - \beta \sum_{n>0} M_{n0} \int \frac{d\omega}{2\pi} \frac{P_0 S(\omega) - P_n S(-\omega)}{\omega_{n0} + \omega} \\ &\quad \cdot \int \frac{d\omega}{2\pi} \frac{S(\omega) [1 - \beta(\omega_{n0} + \omega)] - (P_n/P_0) S(-\omega)}{(\omega_{n0} + \omega)^2}. \end{aligned} \quad (60)$$

Next, we symmetrize this equation by using the fact that $\sum_{m>0} P_m = 1 - P_0$:

$$\begin{aligned} F^2 &= 1 - \beta \sum_{m>n>0} M_{mn} \int \frac{d\omega}{2\pi} \frac{S(\omega) P_n - S(-\omega) P_m}{\omega_{mn} + \omega} \\ &\quad - \frac{\beta}{2} \sum_{m>0} P_m (M_{mm} - M_{00}) \int \frac{d\omega}{2\pi} \frac{S(\omega) - S(-\omega)}{\omega} \\ &\quad - \sum_{m>0} M_{m0} \int \frac{d\omega}{2\pi} \frac{S(\omega) [1 - \beta(\omega_{m0} + \omega)] - (P_m/P_0) S(-\omega)}{(\omega_{m0} + \omega)^2} \\ &\quad - \sum_{m>0} M_{m0} \int \frac{d\omega}{2\pi} \frac{\beta(\omega_{m0} + \omega) [P_0 S(\omega) - P_m S(-\omega)]}{(\omega_{m0} + \omega)^2}. \end{aligned} \quad (61)$$

Note that each line in Eq. (61) has the form $S(\omega)/\omega$ at large ω and hence diverges together with the high-frequency cutoff in the used model of environmental noise (see below). When all the states of the qubit system are included, these divergences cancel each other. However, only part of the eigenstates are used in the numerical calculations, so the divergence does not vanish if one employs directly Eq. (61).

Using the property $\sum_n |\langle n | \sigma_j^z | m \rangle|^2 = 1$, it can be shown that

$$\begin{aligned} \sum_{m>0} P_m (M_{mm} - M_{00}) &= \sum_{m>0} M_{m0} (1 - P_0 - P_m) \\ &\quad - \sum_{m>n>0} (P_m + P_n) M_{mn}. \end{aligned} \quad (62)$$

Combining (61) and (62), we get the final result for fidelity:

$$F^2 = 1 - \int \frac{d\omega}{2\pi} f(\omega),$$

or, in our perturbation approximation,

$$F = 1 - \frac{1}{4\pi} \int d\omega f(\omega), \quad (63)$$

with

$$f(\omega) = \beta \sum_{m>n>0} M_{mn} f_{mn}(\omega) + \sum_{m>0} M_{m0} g_m(\omega).$$

Here

$$\begin{aligned}
f_{mn}(\omega) &= \frac{S(\omega)P_n - S(-\omega)P_m}{\omega_{mn} + \omega} - \frac{P_m + P_n}{2} \\
&\times \frac{S(\omega) - S(-\omega)}{\omega}, \\
g_m(\omega) &= \frac{[1 + (P_0 - 1)\beta(\omega_{m0} + \omega)]S(\omega)}{(\omega_{m0} + \omega)^2} \\
&- \frac{[1 + P_0\beta(\omega_{m0} + \omega)](P_m/P_0)S(-\omega)}{(\omega_{m0} + \omega)^2} \\
&+ \beta \frac{1 - P_0 - P_m}{2} \frac{S(\omega) - S(-\omega)}{\omega}. \quad (64)
\end{aligned}$$

One can see that

$$f_{mn}(\omega) \rightarrow P_n S(\omega) + \frac{P_m + P_n}{2} \frac{S(\omega) + S(-\omega)}{\omega}$$

as $\omega \rightarrow -\omega_{mn}$, and

$$g_m(\omega) \rightarrow \beta^2(P_0 - 1/2)S(\omega) + \beta \frac{1 - P_0 - P_m}{2} \frac{S(\omega) - S(-\omega)}{\omega}$$

as $\omega \rightarrow -\omega_{m0}$. This implies that the poles are removed and the $S(\omega)/\omega$ divergence at infinity also disappears for each term, thus improving the convergence properties of this expression for the numerical evaluation of fidelity.

A. Noise spectral density

For numerical calculations in this paper, we consider the flux noise in aa rf-SQUID. The noise operator $q = I_p \delta \Phi_x$ is therefore related to the flux noise $\delta \Phi_x$ through the rf-SQUID, where I_p is the persistent current of the rf-SQUID. The noise is characterized by its correlation function through the spectral density

$$S(\omega) = \int_{-\infty}^{\infty} dt e^{i\omega t} \langle q(t)q(0) \rangle = I_p^2 S_\Phi(\omega) \quad (65)$$

where

$$S_\Phi(\omega) = \int_{-\infty}^{\infty} dt e^{i\omega t} \langle \delta \Phi_{1x}(t) \delta \Phi_{1x}(0) \rangle \quad (66)$$

is the spectral density of the flux noise. Since the actual noise is of the form of flux noise, the spectral density, $S(\omega) \propto I_p^2$, should depend on the bias point through I_p . Then,

$$S(\omega) = \kappa \left[\frac{\gamma^2}{|\omega|} + \hbar^2 \frac{\eta \omega e^{-|\omega|/\omega_c}}{1 - e^{-\hbar\omega/k_B T}} \right], \quad (67)$$

with

$$\kappa = (I_p/I_{pm})^2, \quad (68)$$

where I_{pm} is the maximum value for I_p , η is a dimensionless coefficient characterizing the Ohmic noise and γ is an energy scale characterizing the $1/f$ noise.

In the actual quantum annealing system described by Eq. (1) of the main text, the persistent current I_p and the tunneling amplitude of qubits are time-dependent. As described in Ref. 18 of the main text, the energy scale $B(s)$ depends on I_p as $B(s) = M_0 I_p^2$, where M_0 is the maximum mutual inductance between the qubits through the tunable couplers and $s = t/t_f$. Therefore, one can write $\kappa(s) = B(s)/B(s_m)$, where $B(s_m) = M_0 I_{pm}^2$. It is therefore sufficient to determine s_m to calculate $\kappa(s)$ at all s .

Measurement of the $1/f$ noise reveals a flux noise spectral density of the form $S_\Phi(2\pi f) = A^2/|f|^\alpha$, with $\alpha \approx 1$. From (65) we find

$$\gamma \approx \sqrt{2\pi} I_{pm} A. \quad (69)$$

For the qubits in the current D-Wave processors we have $\eta \approx 0.1$, $A \approx 3\mu\Phi_0$, and $I_{pm} \approx 1 \mu\text{A}$ at $s_m = 0.636$, which gives $\gamma/h \approx 23 \text{ MHz} \approx 0.02 \text{ GHz}$.